

## Characterization of the superconducting microwave properties of aluminum manganese

M. Lisovenko<sup>1</sup> · Z. Pan<sup>1</sup> · P. S. Barry<sup>1,2,3</sup> · T. Cecil<sup>1</sup> · C. L. Chang<sup>1,2,3</sup> · J. Hood<sup>1,2,3,4</sup> · J. Li<sup>1</sup> · V. Novosad<sup>5</sup> · G. Wang<sup>1</sup> · V. Yefremenko<sup>1</sup>

the date of receipt and acceptance should be inserted later

**Abstract** A Microwave Kinetic Inductance Detector (MKID) is a superconducting pair breaking detector that offers a number of unique advantages for realizing large-format arrays of ultra-sensitive detectors, such as inherent multiplexibility and relative ease of fabrication. With the detection threshold being set by the Cooper pair binding energy, and correspondingly, the superconducting critical temperature ( $T_c$ ), typically well-understood MKID materials such as aluminum (Al) present a lower limit on the operating frequency. Aluminum manganese (Al-Mn) is a promising candidate material for MKIDs because it can be fabricated with nearly identical processing as pure Al, but allows for control of the  $T_c$  with varying levels of Mn doping or post-deposition heat treatment. We present initial results from an early characterization of AlMn using a series of lumped-element superconducting microwave resonators, including measurements of  $T_c$ , internal quality factor, and noise performance over a range of Mn doping.

**Keywords** MKID, Al-Mn, quality factor

### 1 Introduction

Microwave Kinetic Inductance Detectors (MKIDs) are a class of superconducting pair breaking detectors that have a number of unique advantages for realizing large-format arrays of ultra-sensitive detectors [1]. Each MKID is formed from a superconducting resonator that can be tuned to a unique resonant frequency through modification of the device geometry. By placing numerous MKIDs with different resonance frequencies on a single feedline, large numbers of MKIDs can be multiplexed in the frequency domain using minimal cryogenic complexity. The critical temperature ( $T_c$ ) of the superconducting films used for the MKID determines a lower limit on the operating frequency; for example, thin-film aluminum (Al) with a  $T_c \sim 1.3$  K is sensitive to frequencies above  $\sim 90$  GHz. To extend the operating range

---

<sup>1</sup> High Energy Physics Division, Argonne National Laboratory, Lemont, IL 60439, USA

<sup>2</sup> Kavli Institute for Cosmological Physics, University of Chicago, Chicago, IL, 60637, USA

<sup>3</sup> Department of Astronomy and Astrophysics, University of Chicago, Chicago, IL, 60637, USA

<sup>4</sup> Vanderbilt University, Nashville, TN 37235, USA

<sup>5</sup> Materials Science Division, Argonne National Laboratory, Lemont, IL 60439, USA

of MKIDs for use at even lower frequencies, a reliable way of depositing films with a controlled  $T_c$  below 1 K is needed. Doping Al with Mn impurities (hereafter Al-Mn) has been shown to be an effective method for modifying the  $T_c$  of Al, and is now a widely used material for arrays of transition edge sensor bolometers [2, 3, 4, 5, 6]. It has, however, been less studied as a material for use in MKIDs. Manganese, as magnetic material, could affect the quality of the MKID devices. Early studies of Al-Mn MKIDs suggest that at the low doping levels of Al-Mn used for many devices, manganese loses its magnetic characteristic, and the resulting films have been shown to retain a sharp density of states, with only a slight broadening of the superconducting gap, as expected for non-magnetic impurities [7, 8, 9, 10]. In Jones et al. [7], lumped-element kinetic inductance detectors (LEKIDs) have been fabricated using Al-Mn (900 ppm) films with a  $T_c$  of  $\sim 700$  mK. Those LEKIDs demonstrated high quality factors  $\sim 10^5$  and suggested that Al-Mn films have the potential to be used for future instrumentation. In this paper we examine the performance of KIDs fabricated from Al-Mn films with higher doping levels, and correspondingly lower  $T_c$ , that would enable sensitivity at lower frequencies.

## 2 Fabrication

Al-Mn films were deposited by sputtering in a DC confocal magnetron system. High purity Al and Al-Mn (1050, 1150, and 2000 ppm doping level) targets were used for preparing the thin films and sputtered in ultra-high purity argon. The films were deposited onto 6-in diameter silicon (100) wafers at room temperature. For better film quality, all depositions were carried out with a base pressure of  $2 \times 10^{-8}$  Torr or lower. Confocal 3-inch diameter targets and rotation of the substrate holder allowed us to achieve a film thickness uniformity of  $\pm 2\%$  across the 6-in wafers. All films were deposited with a target thickness of 40 nm. Low power (25 W) Ar plasma cleaning of the substrates was done before film deposition to remove contamination from the wafer surface. The single-layer films were fabricated into LEKIDs using contactless photolithography (Heidelberg MLA) followed by wet etching in Transene Type A Al etchant.

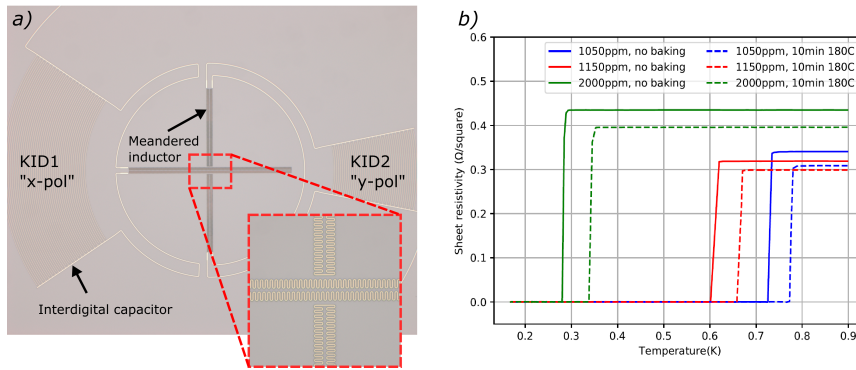


Fig. 1: Left: Photo of a fabricated Al-Mn LEKID Pixel. Right: Sheet resistivity vs. temperature curves for DC  $T_c$  samples with different Mn-doping level and heat treatment.

The LEKID design consists of interdigitated fingers for capacitors and a meander inductor, as shown in the left panel of Fig. 1. Two resonators are interlocked to form a single pixel, with their inductors forming an orthogonal antenna. The resonators were designed to serve as direct absorbing detectors that can be coupled to free space via a feedhorn and waveguide coupling scheme. The resonators are capacitively coupled to a microstrip feedline with five pixels (ten resonators) coupled to a single feedline. In addition to the LEKIDs, each wafer has  $T_c$  test structures that consist of narrow wires that are used to measure the DC resistance of the films as function of temperature in order to determine  $T_c$  and sheet resistivity of the films. The  $T_c$  of the Al-Mn films is sensitive to post-deposition heat treating in addition to the Mn doping level [11]. To investigate the impact of heat treatment on the performance of the Al-Mn films as KIDs we baked a few individual resonator chips and  $T_c$  chips at 180 C for 10 minutes, following the process used in the development of our Al-Mn TESs [12]. In addition to the Al-Mn devices, we also fabricated and tested Al devices to serve as a reference.

### 3 Testing

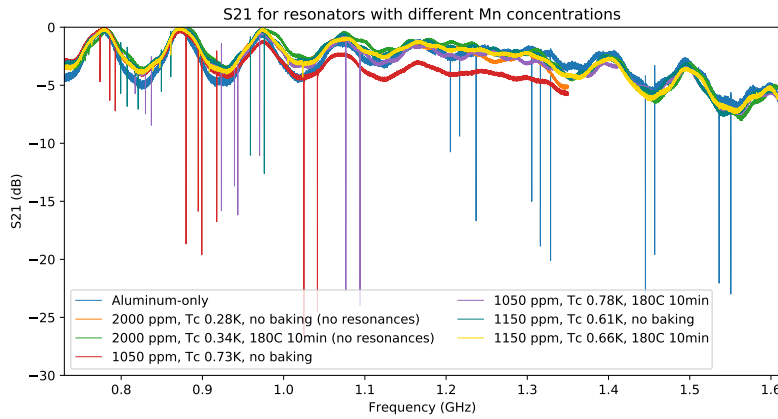


Fig. 2:  $S_{21}$  magnitude vs. frequency for samples with different Mn doping concentrations and different heat treatments (DR base temperature 10 mK). Increasing the Mn concentration decreases the  $T_c$  [11] and shifts the resonance frequency down, which is also illustrated in Fig. 3c. Heating the wafer results in higher  $T_c$  and higher resonance frequencies. No resonances appear in the LEKIDs made with 2000 ppm Al-Mn, which may be due to bifurcation of the resonance at the power levels used in the measurement. Another notable feature is that the 1150 ppm resonances are shallower than the Al and 1050 ppm Al-Mn resonances and become shallower after baking, which is consistent with the low  $Q_i$  values for these samples from Fig. 3a.

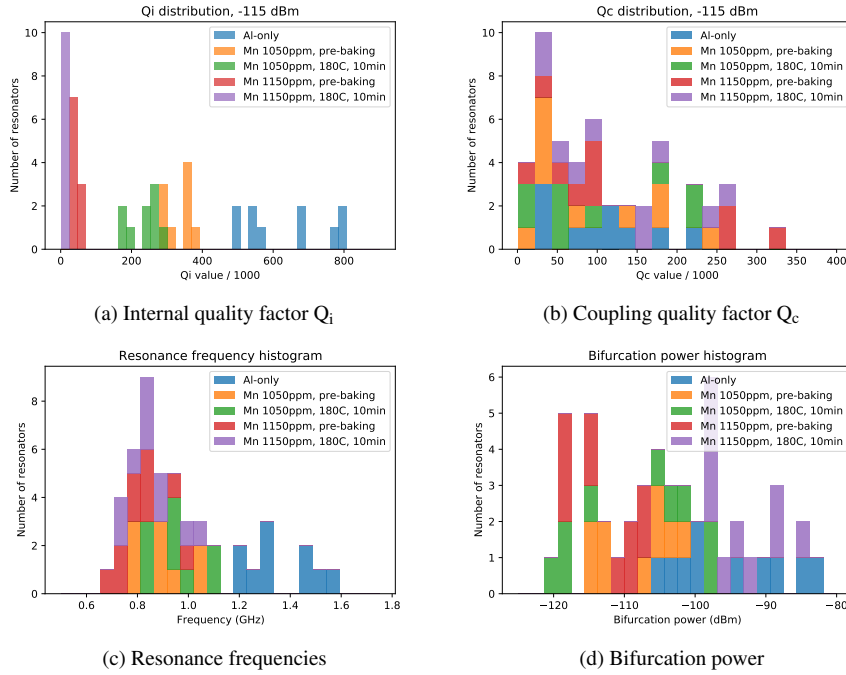


Fig. 3: Histograms of the internal quality factors  $Q_i$ , coupling quality factors  $Q_c$ , resonance frequencies, and bifurcation powers. All data was taken with a Metglas magnetic shield at 10 mK, the base temperature of the measurement cryostat.

Our samples were characterized in a BlueFors dilution refrigerator (DR) with a base temperature of 10 mK. The  $T_c$  samples were mounted to an aluminum sample box and connected via wire bonds to a custom PCB for four-wire resistance measurements. The plate was bolted to the mixing chamber stage of the DR. Resistance measurements were taken using a bias current of 3  $\mu$ A with a temperature sweep rate of 5 mK/min. Resistance versus temperature curves for the Al-Mn films are shown in Fig. 1 (right). As expected, the transition temperature decreases with increasing Mn doping. The measured  $T_c$  are 0.73, 0.61, and 0.28 K for Mn doping of 1050, 1150, and 2000 ppm, respectively. Following baking at 180 C for 10 minutes, the transition temperature for the samples is shifted up roughly 40-60 mK. The transition temperature of the 2000 ppm films suggests a LEKID fabricated from that film should be sensitive to frequencies down to 20 GHz.

The LEKID samples were mounted in an Al sample box that was wrapped in Metglas magnetic shield before being screwed on the cold stage of the DR. Transmission measurements were taken using a VNA. The microwave signal is attenuated and heat sunk at each stage in the DR with a total attenuation of 70 dB before the sample box. After probing the resonators, the signal is amplified using a HEMT. Broad frequency sweeps for each sample are shown in Fig. 2. The shift to lower resonance frequencies in the Al-Mn films due to a reduced  $T_c$  can clearly be seen. Baking the sample increases the  $T_c$  and shifts the resonances to slightly higher frequencies. The yield of the resonators is 100%, 90%, 100%, and 0% for the resonators with 0, 1050, 1150, and 2000 ppm Mn, respectively. The yield after baking is the same as the yield before baking for all of the Al-Mn devices.

Individual S21 resonance curves were fit to determine resonator properties such as the internal quality factor and bifurcation power. The bifurcation power is the driving power on the detector feedline. In Fig. 3a we plot histograms of the key resonator parameters: internal quality factor ( $Q_i$ ), coupling quality factor ( $Q_c$ ), resonance frequency ( $f_r$ ), and bifurcation power.  $Q_i$ ,  $Q_c$ , and  $f_r$  are determined from the fits to the frequency sweeps. The bifurcation power - the power level at which the resonance curve starts to have discontinuity, was determined by inspecting the resonance shape. As seen in Fig. 3a,  $Q_i$  decreases with increasing doping level. Comparing the  $Q_i$  values for baked versus unbaked films, we see that the baked films have lower  $Q_i$  despite having higher  $T_c$ . In Fig. 4a, we plot resonator  $Q_i$  versus reduced temperature,  $x = T/T_c$ . Our measurements show that each Mn doping level follows its own  $Q_i$  vs.  $x$  relationship. The measurements for the aluminum resonator in Fig. 4a (black lines) were done without the Metglas magnetic shield, while all other measurements in this paper were done with magnetic shield. We found that including the magnetic shield increases the  $Q_i$  values by  $\times 2$ , and the lack of magnetic shield can limit  $Q_i$  for the Al-only samples (black lines) towards the low temperature. The fact that the curves in Fig. 4a for different samples do not overlap indicates doping does not simply lower the  $T_c$  from a perfect BCS superconductor, and there may be subgap states [8]. We also measured noise spectra for the 1050 ppm Mn pre-baking device and plotted them in Fig. 4b. Our noise data exhibits features that are characteristic of generation-recombination noise.

Fig. 3b shows that the coupling quality factor  $Q_c$  does not have a strong dependence on doping or baking. We are exploring the source of the large spread in measures  $Q_c$ . A similar spread is seen in devices made using Al and Nb, suggesting it arises from the design of the array rather than the AlMn material. From Fig. 3c, the resonance frequencies clearly decrease with  $T_c$ . Fig. 3d presents the bifurcation powers for our devices and suggests a general decrease in bifurcation power with increased doping. This could explain the unobserved resonances for the 2000 ppm resonators, which could have bifurcation powers below the lower limits of our measurement setup (-120 dBm). Baking increases the  $T_c$  and the bifurcation power. We noticed that the bifurcation power for the 1150 ppm device increased more compared to 1050 ppm after baking, which can be correlated with the small  $Q_i$  after baking (see Fig. 3a).

## 4 Conclusions

We present results from early characterization of superconducting resonators made from Al-Mn. For 1050 ppm Al-Mn, we measure internal quality factors  $> 250K$ , suggesting that these films may be suitable for sensing applications. We have measured resonators with different doping levels, demonstrating correlations among parameters, such as  $T_c$ - $Q_i$ ,  $T_c$ -resonance frequency, and baking- $Q_i$  correlations. The noise measurements show that the resonators are limited by generation-recombination noise. We also found evidence that Mn doping does not simply reduce the  $T_c$  from a perfect Al BCS superconductor.

**Acknowledgements** Work at Argonne, including use of the Center for Nanoscale Materials, an Office of Science user facility, was supported by the U.S. Department of Energy, Office of Science, Office of Basic Energy Sciences and Office of High Energy Physics, under Contract No. DE-AC02-06CH11357. Zhaodi Pan is supported by ANL under award LDRD-2021-0186.

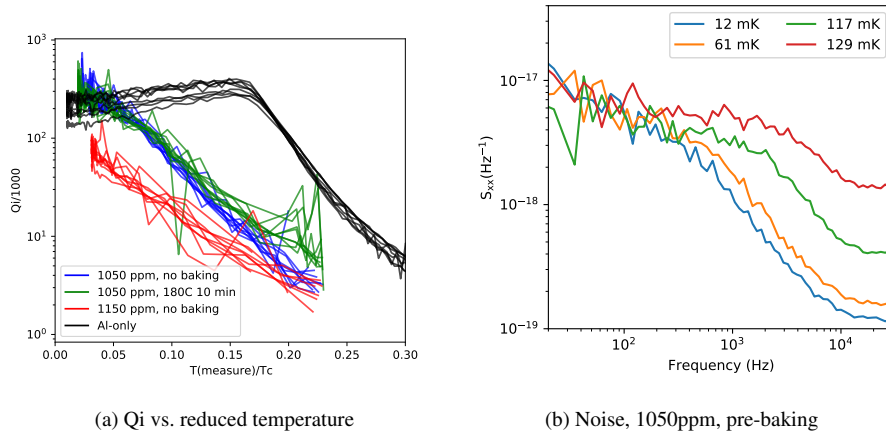


Fig. 4: Left: the internal quality factor vs. reduced temperature (measurement temperature /  $T_c$ ) for resonators with different doping levels and heat treatments. There are some noise scatter in the parameter fits, especially at higher temperatures where the responsivity reduces. Right: noise for the 1050ppm resonator with no baking. The noise shelf and roll-off from generation-recombination are visible.

## References

1. P. K. Day, H. G. LeDuc, B. A. Mazin, A. Vayonakis, and J. Zmuidzinas, “A broadband superconducting detector suitable for use in large arrays,” *Nature*, vol. 425, pp. 817–821, oct 2003.
2. S. W. Deiker, W. Doriese, G. C. Hilton, K. D. Irwin, W. H. Rippard, J. N. Ullom, and L. R. Vale, “Superconducting transition edge sensor using dilute almn alloys,” *Applied Physics Letters*, vol. 85, no. 11, 2004.
3. Y. Lv, H. Huang, T. You, F. Ren, X. Ou, B. Gao, and Z. Wang, “Realization of precise tuning the superconducting properties of mn-doped al films for transition edge sensors,” *Journal of Low Temperature Physics*, vol. 202, pp. 71–82, 2021.
4. S. T. Ruggiero, A. Williams, W. H. Rippard, A. Clark, S. W. Deiker, L. R. Vale, and J. N. Ullom, “Dilute al-mn alloys for low-temperature device applications,” *Journal of Low Temperature Physics*, vol. 134, no. 314, pp. 973–984, 2004.
5. D. R. Schmidt, H. M. Cho, J. Hubmayr, *et al.*, “Al-mn transition edge sensors for cosmic microwave background polarimeters,” *IEEE Transactions on Applied Superconductivity*, vol. 21, pp. 196–198, 2011.
6. E. M. Vavagiakis, N. F. Cothard, J. R. Stevens, C. L. Chang, M. D. Niemack, G. Wang, V. G. Yefremenko, and J. Zhang, “Developing almn films for argonne tes fabrication,” *Journal of Low Temperature Physics*, vol. 199, pp. 408–415, 2019.
7. G. Jones, B. R. Johnson, M. H. Abitbol, *et al.*, “High quality factor manganese-doped aluminum lumped-element kinetic inductance detectors sensitive to frequencies below 100 ghz,” *Applied Physics Letters*, vol. 110, no. 222601, 2017.
8. G. C. Neil, D. R. Schmidt, N. A. Tomlin, and J. N. Ullom, “Quasiparticle density of states measurements in clean superconducting almn alloys,” *Journal of Applied Physics*, vol. 107, no. 093903, 2010.

9. Gallinaro and C. Rizzuto, "Effect of transition metal impurities on the critical temperature of superconducting al, zn, in, and sn," *Physical Review B*, vol. 148, pp. 353–361, 1966.
10. F. T. Hedgcock and P. L. Li, "Magnetic susceptibility of dilute al-mn alloys," *Physical Review B*, vol. 2, no. 5, 1970.
11. D. Li, J. E. Ausermann, J. A. Beall, D. T. Becker, S. M. Duff, P. A. Gallardo, S. W. Henderson, G. C. Hilton, S.-P. Ho, J. Hubmayr, *et al.*, "Almn transition edge sensors for advanced actpol," *Journal of Low Temperature Physics*, vol. 184, no. 1, pp. 66–73, 2016.
12. A. J. Anderson *et al.*, "Performance of Al-Mn Transition-Edge Sensor Bolometers in SPT-3G," *Journal of Low Temperature Physics*, vol. 199, pp. 320–329, Apr. 2020.

### **Ethics declaration**

Competing interests

The author declare no competing interests.